Static & Transient Cavitation Threshold Measurements for Mercury

by

F. Moraga*, R. P. Taleyarkhan
Oak Ridge National Laboratory
Oak Ridge, Tennessee, 37831, USA
(*) - Oak Ridge Associated Universities
Oak Ridge, TN, USA

ABSTRACT

Transient and static cavitation thresholds for mercury as a function of the cover gas (helium or air), and pressure are reported. Both static and transient cavitation onset pressure thresholds increase linearly with cover gas pressure. Additionally, the cavitation thresholds as a function of dissolved gases were also measured and are reported.

INTRODUCTION

The use of mercury as a target of a proton beam for accelerator-driven neutron sources, such as the Spallation Neutron Source (SNS)[1], has created the need of measuring its cavitation threshold. For SNS, enormous local temperature rise-rates (~10^7°C/s) are expected during the brief beam pulse (~0.5 μs). This phenomenon gives rise to fluid pressure oscillations that can be as high as +/- 30MPa. As is well-known, large-enough tensile (i.e., negative) pressures can give rise to onset of fluid cavitation. Since the flow field and shock loadings on structures can be strongly influenced by cavitation onset, a focussed study was undertaken to evaluate cavitation onset thresholds under SNS specific conditions.

The static cavitation threshold of mercury in contact with Pyrex glass has been measured by Briggs[2], who obtained values ranging from -7 to -425 bars for cavitation onset in mercury in a glass spinner apparatus. The variation was directly traceable to heat treatment of the glass capillary tubes during gas evacuation from the tubes. Briggs employed extreme measures such as placing his apparatus in a furnace at 500 °C for extended periods of time, and torching of the capillary tubes. Such extreme measures are not practically feasible to employ for SNS operating conditions; and hence, were not employed. Given the importance of pressure transients in the SNS, it was necessary to measure the mercury cavitation threshold under transient conditions also.

In this work, we report static and transient cavitation threshold measurements of mercury as a function of the cover gas pressure and the gas content for both, helium and air. For transient cavitation, the measurement method is very similar to that used by Galloway[3] and West[4,5] to measure acoustically induced cavitation in several liquids.

STATIC CAVITATION SETUP

The basic apparatus used to conduct static cavitation onset experiments utilized a spinner apparatus which has been described elsewhere[6]. Unlike the apparatus used in Ref. 6, in order to be able to pressurize the mercury, a valve was mounted on top of the glass spinner. Figure 1 shows a picture of the modified glass spinner. The valve on top and the mercury filling the two lower arms of the glass spinner are clearly visible. As indicated in Figure 1, the distance between the mercury meniscus in each arm is 26.8 cm. As this piece of glassware rotates at an angular speed measured independently by a strobe light and a magnetic tachometer, the mercury at the lower central part of the spinner experiences a tensile state. When the tensile pressure reaches the cavitation threshold, a bubble forms in the fluid at the junction between the arms. Knowing the angular speed of the spinner at the moment of the bubble formation, ω, the separation radius, r, and height, h, of the mercury column and the static pressure, P_0, at the mercury-helium interface, the cavitation onset pressure, P, can be calculated as,

$$P = P_0 + \rho g h - \rho r^2 \omega^2/2. \qquad (1)$$

The glassware was cleaned with acetone before filling it with mercury. Additionally, the sides were heated to minimize nucleation sites before starting the

measurements, but not in between measurements. In the past[6], we found that once mercury was in the glass container, torching has limited ability to remove nucleation sites, presumably because of poor wettability. In contrast, Briggs[2] applied heat treatments while making a vacuum in the glass tubes. Before measurements, the mercury was subjected to a given static pressure for at least half an hour, to reach the equilibrium dissolution level.

DYNAMIC CAVITATION SETUP

The chamber was a 6.6 cm outer diameter (OD) glass sphere custom blown to be of spherical shape. The neck of the sphere was made to accept a "00" stopper in such a way that the base of the stopper was flush with the interior sphere surface. At the midsection of the sphere and concentric with the stopper axis (see Figure 2), a cylindrical piezoelectric ceramic transducer was cemented to the sphere. The dimensions of this transducer are 7.6 cm OD, 6.6 cm ID and 2.5 cm height. It was used to drive power into the chamber.

A small piezoelectric ceramic disk of 3 mm OD was glued to the glass equidistant from the neck and the driving transducer. This small transducer acted as a microphone and from here on will be referred to as the pill microphone (PM). The signal of this (PM) was used to determine cavitation occurrence at the center of the chamber.

Before filling the chamber, acetone was used to clean it thoroughly. A 100 watt audio amplifier was the source of power. In order to increase the output voltage given to the piezoelectric ceramic transducer, inductors were added to form a series resonant circuit at the resonant frequency of the chamber, 24.620 KHz. Once the electric resonance was optimized, there was enough power available to measure the cavitation threshold up to 3.1 bars of hydrostatic pressure, P_0, in a helium atmosphere. The maximum driving voltage reachable was 370 V.

DYNAMIC CAVITATION EXPERIMENTAL PROCEDURE

The cavitation threshold is determined from the following formula,

$$P=P_0 - V_{PZT}/K, \qquad (2)$$

where, P_0 is the static pressure in the chamber, V_{PZT} is the root mean square voltage measured at the driving transducer before the fluid cavitates and K is a proportionality constant that was determined experimentally. The experimental method implicit in equation (2) has been successfully used previously to measure acoustically induced cavitation thresholds of several liquids[3-5].

A Precision Acoustics™ needle hydrophone was used to map the pressure profile in the chamber. As shown in Figure 3, we found that the ratio of pressure amplitudes between the maximum pressure location in the interior, and the pressure corresponding to a location close to the edge was 18.

For analytic quantification, the CTH shock dynamics code[7] was used (as has been done previously for shock physics modeling of SNS target systems[8]) to model the dynamic response of the spherical glass chamber and wave focusing in mercury. The model incorporates a quartz sphere filled with mercury. Figure 3 displays the peak pressure values at locations along the radius for the numerical and experimental data taken with the needle hydrophone. For both sets of data the amplification factor at the center is ~18. Similar numerical results were obtained at other values of pre-stressed states for the quartz wall. This comparison provided an excellent cross-check and confidence in the use of the amplification factor of 18 for mercury; for estimating pressures at the onset of cavitation.

Since mercury is not transparent, it was not possible to visualize where or when cavitating bubbles were formed. Therefore, we relied mainly on the output of the pill microphone to determine that the fluid was cavitating. Figure 4 shows typical pill microphone outputs for a cavitating and a non-cavitating fluid. Other indicators of cavitation were a sudden drop of the driving voltage, V_{PZT}, and an audible hissing noise. These other two indicators have been described in the past by other researchers[3-5] working with transparent fluids. The sudden voltage drop and the audible noise were present only with waveforms similar to the cavitating waveform shown in figure 4. Moreover, in preliminary experiments conducted with 18 MΩ/cm distilled water, cavitation bubbles were observed in the bulk of the fluid only for waveforms similar to the cavitating waveform in figure 4 while simultaneously, both, the characteristic audible noise and voltage drop were also observed.

The cavitation threshold was determined as a function of pressure and as a function of gas concentration for helium and air, always at room temperature, (approximately 25 °C). Before a given measurement, the chamber was maintained under pressure for at least an hour, and sometimes up to fifteen hours at the target pressure while the mercury was driven acoustically at a power level that produced negligible

heating. Next, the driving voltage was increased in small steps. At each step the behavior of the chamber was observed for at least 60 s. Depending partly on the power level, between 0 and 30 instances of cavitation characterized by short bursts of cavitation lasting less than a second or up to several seconds would be observed. On other occasions, continuous cavitation would be observed immediately after the power level was increased or after a short interval ranging from a few seconds up to a minute. We define continuous cavitation as cavitation occurring for more than 90% of a given time interval of the order of few minutes. After waiting for several hours on occasions, we had observed that once continuous cavitation has set in, the fluid would not leave the continuous cavitation mode as long as the power level was kept constant. Therefore, we found it unnecessary to monitor the system for periods longer than a minute. We define the cavitation threshold as the pressure level at which continuous cavitation occurs. This definition is somewhat arbitrary and less conservative than that adopted by Galloway[3]. We feel that our definition is more appropriate for the type of behavior we observed in our experiments, where a burst mode and a continuous cavitation mode were easily differentiated. In contrast, neither Galloway's experiments with several non-metallic liquids, nor our preliminary experiments with water showed such a clear difference between continuous and burst type cavitation.

EXPERIMENTAL RESULTS

Figure 5 shows the static cavitation data obtained with the spinner apparatus. It is clearly seen that the threshold pressure increases as the static pressure increases. All thresholds occur at positive pressures.

Figure 6 shows the results for acoustically induced transient cavitation as a function of pressure. Not only did the data exhibit a clear linearly increasing trend, but repeatability can be observed. The cover gas, air or helium, has negligible effect on the monitored cavitation threshold.

Figure 7 shows transient cavitation thresholds as a function of the cover gas pressure used to reach the equilibrium dissolution. All the measurements in this figure were acquired at 1 bar static pressure. The pressure in the horizontal axis in figure 7 is the one that was used to reach the equilibrium dissolution concentration of the gas in mercury. This procedure measures the cavitation threshold as a function of the gas content if during the measurements negligible degassing occurs. Unlike the results shown in Fig. 6, a very significant difference is observed between air and helium.

The error range increases from 0.15 to 0.38 bars, increasing as the static pressure increases. The scattering observed in the data is much smaller than the error bars. The main source of error is a 20% uncertainty in the constant K (see Equation 2).

DATA ANALYSIS & CONCLUSIONS

A clear tendency to increase the cavitation threshold with the static pressure or the gas content was observed for both, dynamic and static cavitation. Briggs[2] measured static cavitation thresholds ranging from -7 to -425 bars. The large differences between Brigg's data and that of this work, can be explained considering that Briggs made a vacuum in his glassware before filling it with mercury and experimented with several different heat treatments of the glass surface during the gas evacuation. In contrast, we torched the glass walls when the mercury was already inside the glass container and did not employ elaborate heat treatment procedures.

Differences in the static and dynamic data may be explained by the definition adopted for determining transient cavitation thresholds, the different nature of the pressure transients at which the fluid is exposed and the possible presence of nucleation sites at the glass wall of the spinner apparatus.

The data dispersion for static thresholds is larger than for dynamic thresholds. This fact could be due to the presence of nucleation sites at the glass wall of the spinner apparatus. But it also reflects the fact that the adopted cavitation threshold criterion for the dynamic setup is more quantitative (i.e., it gives more reproducible data).

The similarity between air and helium data as a function of pressure is evident. This suggests that at the equilibrium gas concentration, the effects of air and helium are similar. However, helium seems to get out of solution much faster than air, as is suggested by the gas concentration data.

Galloway[3] found that the acoustically induced transient cavitation threshold of water was independent of the static pressure, P_0. This is not what we found for mercury. This difference suggests that the amount of dissolved gases in mercury is a strongly increasing function of the cover gas pressure and that the amount of dissolved gasses is the main variable controlling the transient cavitation threshold.

The uncertainties in these measurements are more than acceptable for practical application accelerator driven in SNS-type systems where the expected tensile

pressures are more than 100 times the level needed for cavitation onset. However, if smaller errors are desirable, it seems convenient to move to a larger chamber, for which it would be relatively simple to diminish the uncertainties related to 'K'. This will imply the need of a more powerful driving transducer and source of power.

REFERENCES

1. T. A. Gabriel *et al.* "Overview of the SNS target station." *Proc. of Int. Topical Meeting on Advanced Reactor Safety, ARS'97.* Orlando. Florida. 1997.
2. L. Briggs, "The limiting negative pressure of mercury in Pyrex glass", *J. Applied Physics.* **24** No 4, p. 488. April 1953.
3. W. J. Galloway, "An experimental study of acoustically induced cavitation in liquids." *J. Acoustical Society of America.* **26**, No. 5. September 1954.
4. C. West, "Cavitation nucleation by energetic particles", United Kingdom Atomic Energy Authority report,1967.
5. C. West, "Fast neutron detection by ultrasonic cavitation", Ph.D. thesis. University of Liverpool. UK, 1965.
6. R. P. Taleyarkhan et al., "Experimental determination of cavitation thresholds in liquid water and mercury,"*Second Int. Topical Meeting on Nuclear Applications of Accelerator Technology*. Gatlinburg, Tennessee. September 1998. p. 650.
7. J. McGlaun and S. L. Thompson. "CTH: A Three-Dimensional Shock Wave Physics Code." *Int. J. Impact Engr.*, **10**. 1990.
8. R. P. Taleyarkhan *et al.*. "Results of Thermal Shock Modeling and Analysis for the National Spallation Source." *Proceedings of Topical Meeting on Nuclear Applications of Accelerator Technology.*" p. 293-300. November 1997. Albuquerque, New Mexico.

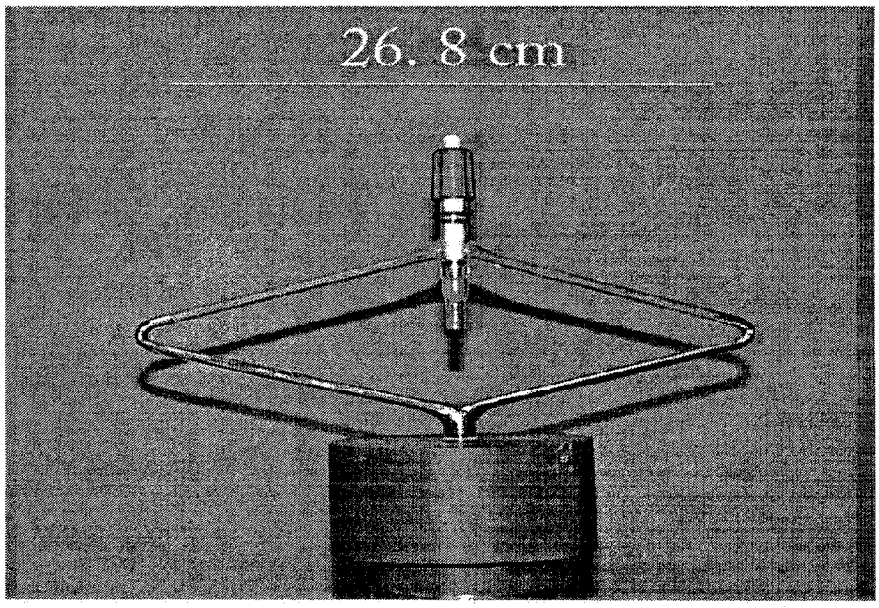

Figure 1. Detail of glass spinner. The distance between the helium-mercury

interfaces in each arm is 26.8 cm.

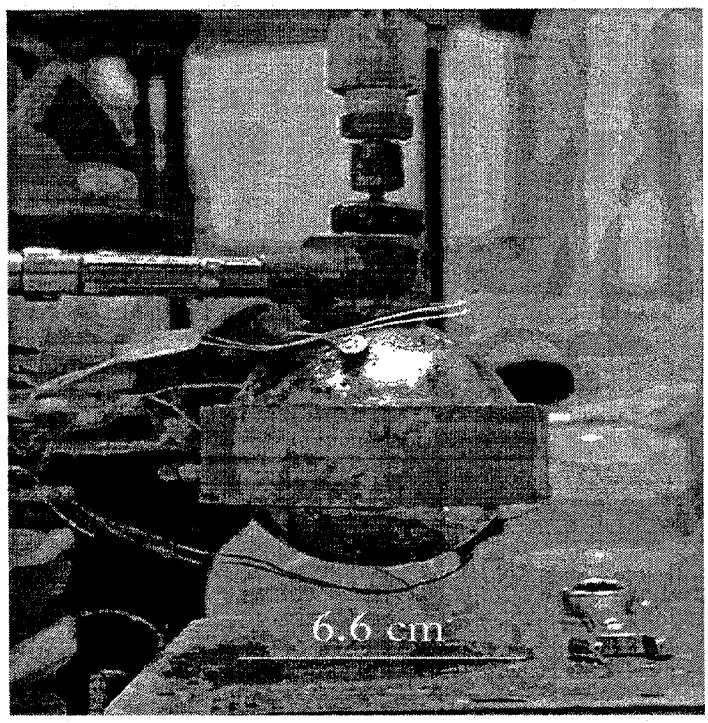

Figure 2 Picture of the resonating chamber. The outside diameter of the glass sphere is 6.6 cm.

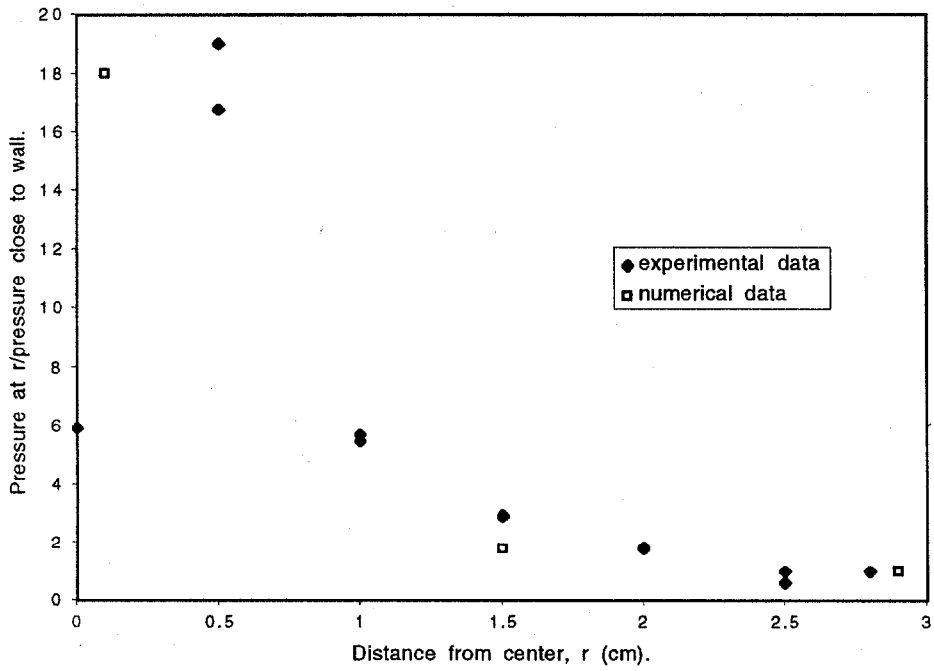

Figure 3 Pressure profile in the resonating chamber.

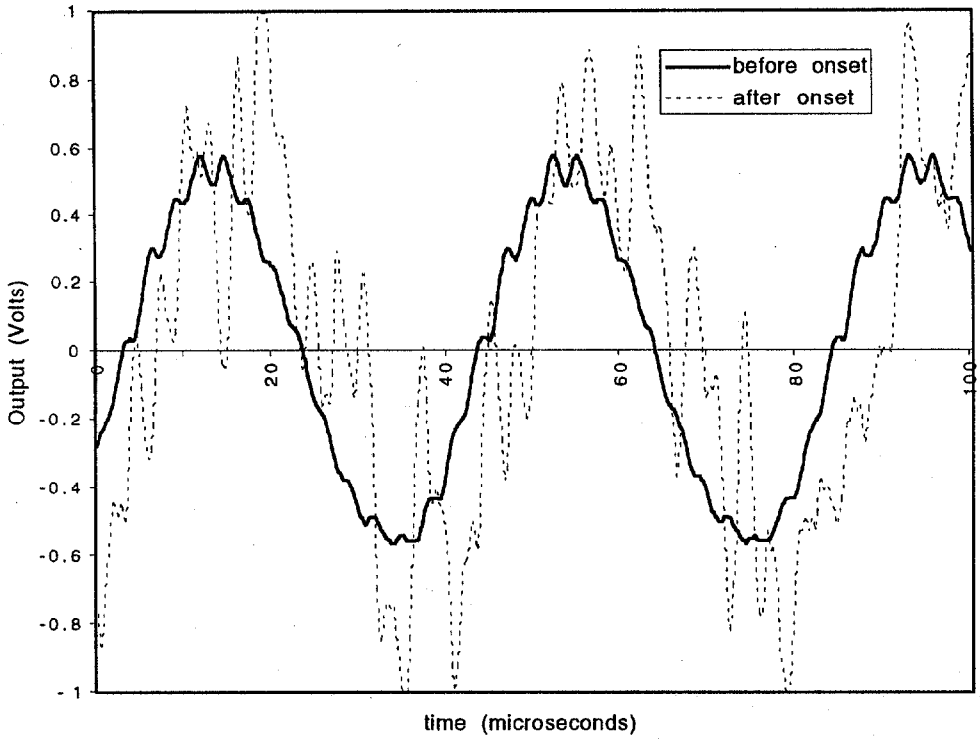

Figure 4. Pill microphone output immediately before and after cavitation onset.

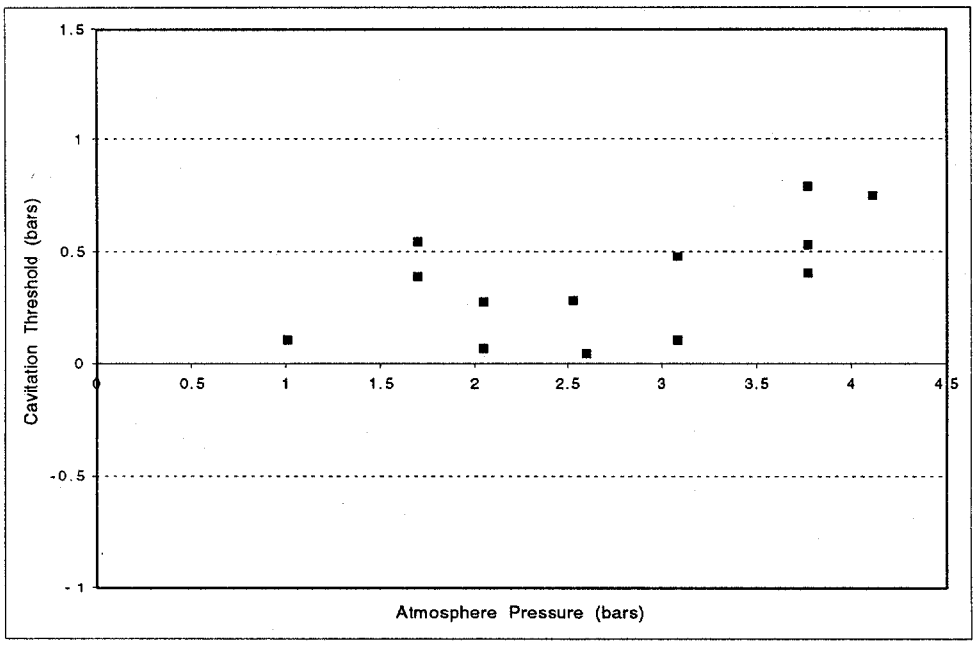

Figure 5 Static cavitation threshold of mercury as a function of helium pressure.

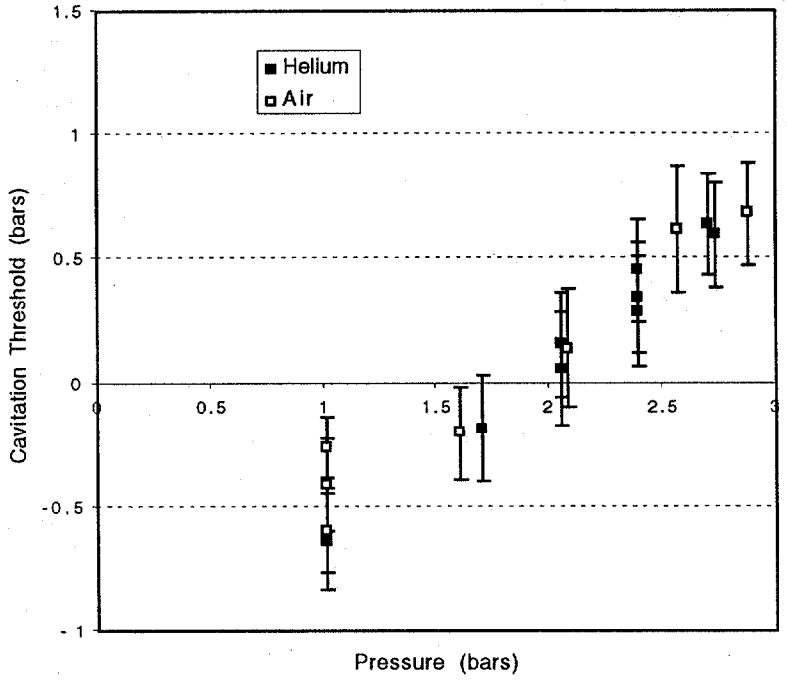

Figure 6 Acoustic transient cavitation threshold of mercury as a function of cover gas pressure for helium and air.

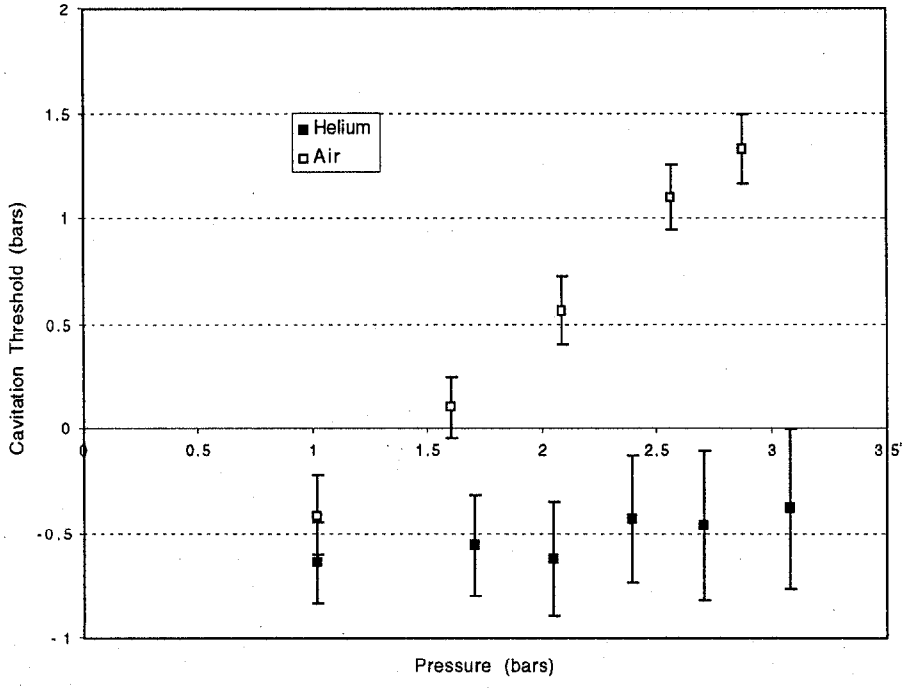

Figure 7 Acoustic transient cavitation threshold of mercury at 1bar cover gas pressure as a function of the initial pressure used to reach the equilibrium gas dissolution.